EVOLUTIONARY BIOLOGY

Visual opsin gene expression evolution in the adaptive radiation of cichlid fishes of Lake Tanganyika

Virginie Ricci[1]*, Fabrizia Ronco[1,2], Nicolas Boileau[1], Walter Salzburger[1]*

Tuning the visual sensory system to the ambient light is essential for survival in many animal species. This is often achieved through duplication, functional diversification, and/or differential expression of visual opsin genes. Here, we examined 753 new retinal transcriptomes from 112 species of cichlid fishes from Lake Tanganyika to unravel adaptive changes in gene expression at the macro-evolutionary and ecosystem level of one of the largest vertebrate adaptive radiations. We found that, across the radiation, all seven cone opsins—but not the rhodopsin—rank among the most differentially expressed genes in the retina, together with other vision-, circadian rhythm–, and hemoglobin-related genes. We propose two visual palettes characteristic of very shallow- and deep-water living species, respectively, and show that visual system adaptations along two major ecological axes, macro-habitat and diet, occur primarily via gene expression variation in a subset of cone opsin genes.

INTRODUCTION

Animals perceive a range of abiotic and biotic environmental cues through one or several of their sensory systems (*1*–*3*). This ability to monitor—and to situationally respond to—their surroundings is key to animal survival, which in turn exposes the different components of sensory systems, and hence the genes and genetic networks underlying them, to strong selection (*4*–*7*).

In many animal species, the visual sensory system is central to a number of vital tasks including orientation, navigation, foraging, predator avoidance, communication, mate choice, and circadian rhythm adjustment (*8*–*10*). The primary sensory organ of the visual system is the eye, which is present—in varying forms and levels of complexity—in almost all animal phyla (*11*–*13*). Eyes convert visual stimuli into neuronal signals. This "phototransduction cascade" is initiated through the light-induced isomerization of a photon-sensitive nonprotein chromophore (retinal) that is covalently bound to a visual opsin protein to form the visual pigment contained in the photoreceptor cells in the retina, the multilayered neural tissue lining the eye's inner surface (*10*, *14*–*17*). The specific waveband of light absorbed by a visual pigment—typically indicated by the maximal spectral sensitivity (λ_{max})—is mainly determined by the type of visual opsin protein (*18*–*20*).

In the vertebrate eye, two basic kinds of photoreceptor cells are present in the retina, the cone photoreceptor cells responsible for photopic (color) vision under bright-light conditions and the rod photoreceptors accounting for scotopic vision in dim light (*14*). At the molecular level, vertebrates are equipped with an ancestral set of five types of visual opsin genes: four cone opsins that form visual pigments sensitive to the ultraviolet (UV) (*SWS1*), the violet-blue (*SWS2*), the green (*RH2*), and the red (*LWS*) wavebands of the light spectrum, plus typically a single rod opsin (*RH1*) [(*10*, *14*, *18*, *19*, *21*, *22*), but see (*23*)]. The evolution of visual opsin genes has been more dynamic in teleost fishes than in other vertebrate clades, which is evident—among other things—from the expansion of the visual opsin gene repertoire to a median number of six cone opsins in teleosts (compared to two to four in most tetrapods) and a record number of 38 rod opsins in the deep-sea silver spinyfin (*10*, *23*–*25*). The greater diversity and complexity of the visual opsin gene repertoire is likely a response to the greater diversity of light environments that fishes are exposed to.

In aquatic environments, light is absorbed and scattered in the water column as a function of wavelength and depth, which is due to the optical properties of water in combination with other factors such as phytoplankton content, dissolved organic matter, and silt (*26*–*28*). In general, a broad-spectral waveband ranging from UV to red light is available in shallow waters, whereas in deeper waters a narrower spectrum remains, with a prevalence of blue and blue-green hues (*27*–*29*). In line with this, many organisms living in the aquatic realm feature specific adaptations of their visual systems that function to better match the ambient light conditions (*10*, *14*, *21*, *23*, *30*–*38*). With respect to teleost fishes, a variety of scenarios have been documented on how they can maximize their visual performance in a given environmental context (*10*, *23*, *32*, *39*). These include adaptive modifications in eye size and/or morphology, lens structure, photoreceptor compositions, and layering of the retina (*40*, *41*); adaptive changes in visual opsin gene sequences (*30*, *37*, *42*); the expansion of the visual opsin gene repertoire coupled with functional diversification (*23*, *24*, *43*–*45*); and changes in expression levels of the different visual opsin genes (*46*–*49*).

Here, we scrutinized the nature of visual adaptations across one of the most notable examples of adaptive radiation and explosive diversification, the cichlid fishes of African Lake Tanganyika (*50*–*53*). Approximately 240 cichlid species have evolved in this lake from a common ancestor in less than 10 million years, occupying a wide range of habitat and feeding niches and varying greatly in species-specific morphological, behavioral, and life-history traits. Cichlids rely, in principle, on a dichromatic to tetrachromatic color vision system and have seven cone opsins plus one rod opsin (Nile tilapia: *SWS1*, λ_{max} = 360 nm; *SWS2B*, λ_{max} = 425 nm; *SWS2A*[α], λ_{max} = 456 nm; *RH2B*, λ_{max} = 472 nm; *RH2A*β, λ_{max} = 517 nm; *RH2A*α, λ_{max} = 528 nm; *LWS*, λ_{max} = 560 nm; *RH1*, λ_{max} = 516 nm) (*10*, *23*, *32*, *54*, *55*). The arrangement of photoreceptor cells in the retina was further shown to vary between

[1]Zoological Institute, Department of Environmental Sciences, University of Basel, Basel, Switzerland. [2]Natural History Museum, University of Oslo, Oslo, Norway.
*Corresponding author. Email: virginie.ricci@unibas.ch (V.R.); walter.salzburger@unibas.ch (W.S.)

cichlid species, resulting in different mosaic arrangements of rods, single and double cones (two joined single cones), with single cones typically expressing short wavelength–sensitive opsins (*SWS1*, *SWS2A*, and *SWS2B*) and double cones expressing medium to long wavelength–sensitive ones (*RH2A*α, *RH2A*β, *RH2B*, and *LWS*) (*10*, *32*, *36*). Among the available visual opsin genes, usually only a subset—often referred to as visual palette—is expressed at a given life stage (*31*, *36*, *39*, *47*, *48*, *54*, *56*, *57*). Since the reinspection of whole-genome data from virtually all cichlid species in Lake Tanganyika (*52*) did not reveal evidence for gene duplications or strong signals of positive selection [$d_N/d_S < 1$, but see (*58*)] in any of the visual opsin genes (see below), we here focused on gene expression dynamics and produced 753 retinal transcriptomes in a phylogenetically, ecologically, and phenotypically representative set of 112 cichlid species endemic to Lake Tanganyika (that is, close to half of the lake's cichlid fauna) to (i) identify likely adaptive changes in the expression of vision-related genes, (ii) define putative visual palettes on the basis of cone opsin expression profiles and reconstruct their evolution, and (iii) test for an association between opsin expression levels and the species' macrohabitat, feeding ecology, as well as a vision-related phenotype, eye size.

RESULTS

To investigate visual opsin and overall retinal gene expression dynamics in the adaptive radiation of cichlid fishes of Lake Tanganyika, we generated 753 transcriptome profiles from retinal tissue of 112 species covering all 12 cichlid tribes endemic to that lake plus one Haplochromini species from the Lake Tanganyika drainage, and one representative each of the more widespread tribes Oreochromini and Tylochromini that are not part of the in situ radiation but colonized the lake secondarily (see table S1 for details on specimens) (*52*). To account for sex and intraspecific differences, we collected at least three males and three females per species, whereby samples were taken at roughly the same time of the day whenever possible. For each specimen, total RNA extracted from the retina of a single eye was sequenced on Illumina NovaSeq 6000 [TruSeq standard protocol with 100 base pairs (bp) paired end; median number of sequenced reads per sample = 19,537,332; fig. S1A and table S2] after RiboZero Gold ribosomal RNA (rRNA) depletion (Illumina). As in our previous work (*59*), the individual RNA reads of every library were mapped to the phylogenetically equidistant—with respect to the ingroup taxa—*Oreochromis niloticus* reference genome (RefSeq accession GCF_001858045.2; female) to infer which genes were expressed and at which levels. After selection of protein-coding and long noncoding RNA (lncRNA) features and removal of lowly expressed genes, the total read count in exonic features ranged from 32,854 to 7,643,707 per library (median = 2,383,349; fig. S1B and table S2), and the number of expressed genes varied from 7952 (27.42%) to 28,068 (96.78%) (median = 22,087, total of 29,002 RNA features; fig. S1C and table S2). The variation in read counts and numbers of expressed genes between samples was mainly explained by differences in the number of sequenced reads and the rRNA contents (fig. S2).

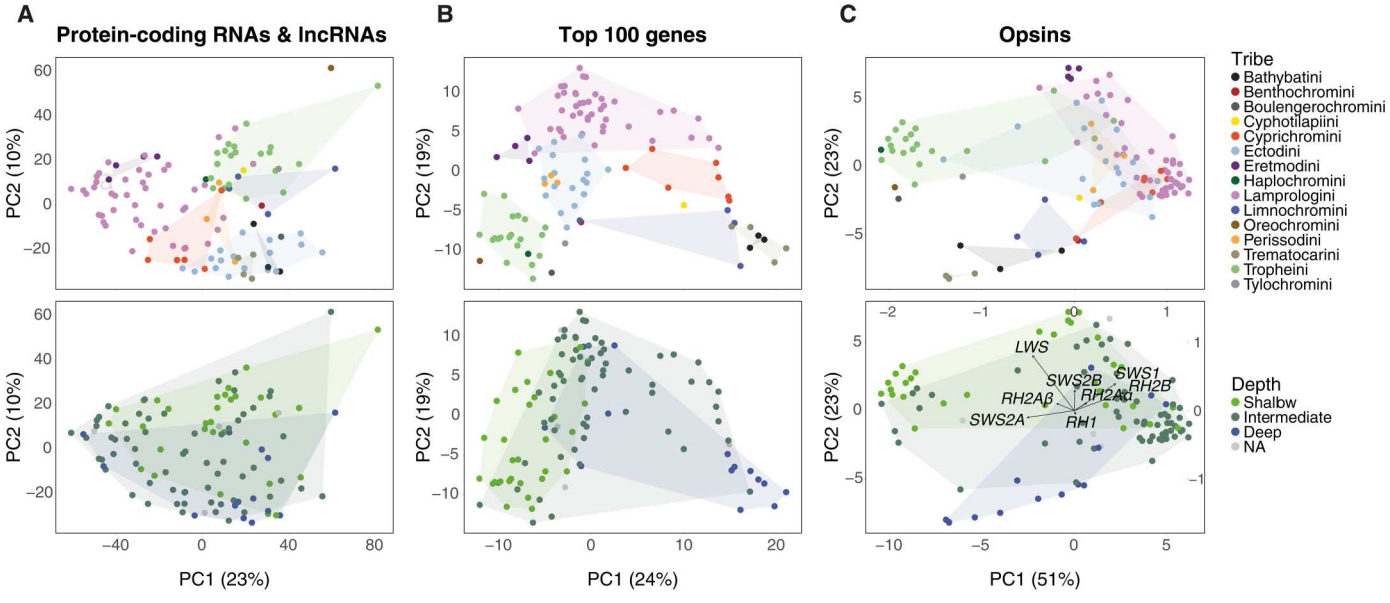

Fig. 1. Retinal gene expression patterns in Lake Tanganyika cichlid fishes. PCAs of (**A**) overall gene expression levels (protein-coding RNAs and lncRNAs combined), (**B**) gene expression levels of the top 100 genes with the greatest variance in gene expression, and (**C**) visual opsin gene expression levels. Each dot represents the weighted mean value of a given species and is color-coded according to the tribe that a species belongs to (top) or the depth category at which a species occurs (bottom; NA indicates that the depth of occurrence is unknown for the species in question, or that the three depth categories do not adequately capture the ecology of a given species). Tribal assignments and tribe color-coding follow (*52*). Tribal and depth ranges are indicated with convex hulls (except for NAs). The loadings of PC1 and PC2 are indicated in the PCA plot of visual opsins color-coded by depth in (C). The variance explained by each principal component is reported in parenthesis. PCA plots of protein-coding RNAs and lncRNAs combined and visual opsins at the individual level are available on Dryad (https://datadryad.org/stash/dataset/doi:10.5061/dryad.r2280gbj2).

The visual opsin gene repertoire of Lake Tanganyika cichlids

Before investigating the expression of visual opsin genes, we confirmed the presence of seven cone opsins (*SWS1*, *SWS2B*, *SWS2A*, *RH2B*, *RH2A*β, *RH2A*α, and *LWS*) and one rhodopsin (*RH1*) in the genomes of Tanganyikan cichlids. A reexamination of the results of our previous gene duplication analysis based on 488 genomes (246 taxa) (*52*) revealed no evidence that any particular visual opsin gene was duplicated in any of the studied cichlid species. When applying our cichlid-tailored opsin raw read mapping approach [results are available on Dryad: https://datadryad.org/stash/dataset/doi:10.5061/dryad.r2280gbj2; for results involving *RH1*, see (*30*)] to the cone opsins, we confirmed the presence of a single copy of each cone opsin gene—complete or "degenerated"—in 517 Lake Tanganyika cichlid genomes (271 species including outgroups). We also reinspected the results of our previous positive selection analysis based on 471 genomes (243 taxa) (*52*) and found no clear signs of positive selection ($d_N/d_S < 1$) in any of the cone opsins across the radiation [for results involving *RH1*, see (*30*)].

Gene expression patterns in the retina of Lake Tanganyika cichlids

To visualize transcriptome-wide patterns of gene expression differentiation in the retinal tissue of Lake Tanganyika cichlids, we performed a principal components analysis (PCA) on the basis of weighted species mean values measured as normalized read counts using the variance stabilizing transformation method (VST; Fig. 1 and fig. S3) (PCA plots at the individual level are available on Dryad: https://datadryad.org/stash/dataset/doi:10.5061/dryad.r2280gbj2). Like in all other tissues investigated so far across the adaptive radiation of cichlid fishes in Lake Tanganyika (*59*), a strong phylogenetic signal was recovered in the retinal gene expression profiles, with species mainly clustering according to tribes and only to a moderate degree according to water depth of occurrence (Fig. 1A). The only representative of the Haplochromini (*Astatotilapia burtoni*) clustered with members of the Tropheini, with whom it shares a common ancestor (*60*). *Oreochromis tanganicae* (Oreochromini) and *Interochromis loocki* (Tropheini) appeared separate from the rest of the species, which was, however, not the case for the phylogenetically most distant species (*Tylochromis polylepis*; Tylochromini), which clustered with Tropheini representatives. The PCA based on protein-coding RNAs alone (25,335 features; fig. S3A) largely recovered the global gene expression patterns, which is not surprising given that protein-coding RNAs accounted for 87.36% of the expressed genes in our dataset. The PCA based on lncRNAs (3667 features; 12.64% of the expressed genes; fig. S3B) recovered an even stronger phylogenetic signal with very little overlap between tribes.

To focus on the most differentially expressed genes in our dataset, we performed PCAs based on the top 100 (Fig. 1B and table S4) and the top 500 genes (fig. S3C) with the greatest variance in gene expression. In both PCAs, species generally clustered by tribe with little (top 100 genes) to moderate (top 500 genes) overlap between tribes. At the same time, we found a clear separation between species with respect to the water depth at which they occur, with little overlap between shallow- and deep-water living species, except for one deep-water species (*Plecodus paradoxus*, Perissodini) that clustered with shallow-water representatives (along PC1 accounting for 24% of the variance in the top 100 genes, Fig. 1B, and PC2 accounting for 16% of the variance in the top 500 genes, fig. S3C). All seven cone opsin genes (but not the rod opsin, *RH1*; table S3) ranked within the top 37 genes with the greatest variance in expression (five of the cone opsins were in the top 12 genes; table S4), with the red-sensitive opsin (*LWS*) being the single-most differentially expressed gene in the retina of Lake Tanganyika cichlids overall. In addition to visual opsins, 14 of the top 100 genes have a known function related to vision, including retinal phosphodiesterase subunit genes and rhodopsin kinases (table S4). Moreover, there were eight hemoglobin subunit genes among the top 18 genes (table S4), indicating that in Tanganyikan cichlids, hemoglobin genes are differentially expressed along the depth gradient. This result is compatible with the finding that hemoglobin genes in Lake Malawi cichlids have experienced divergent selection with respect to depth (*61*, *62*). Since the retinal tissue is avascular in most vertebrates (*63*, *64*), we suspect that the hemoglobin genes are not expressed in the retina itself, but in the blood vessels nourishing it (*65*). Last, five genes with a putative function in circadian rhythm regulation, which also depends on light detection in (cichlid) fishes (*10*, *66*, *67*), ranked among the top 80 genes (table S4).

In a third step, we focused exclusively on the visual opsin gene expression profiles and performed a PCA based on the expression information from the seven cone and the single rod opsins (Fig. 1C) (PCA plots at the individual level are available on Dryad: https://datadryad.org/stash/dataset/doi:10.5061/dryad.r2280gbj2). In the same way as in the PCAs of the top 100 (Fig. 1B) and top 500 (fig. S3C) genes with the greatest variance in gene expression, species clustered according to tribes with overlap between some of the tribes, but also with respect to depth of occurrence (in this case mainly represented by PC2 accounting for 23% of the variance; Fig. 1C).

Opsin expression profiles and visual palettes

To examine interspecific differences in the expression of visual opsin genes, as well as to discriminate between rod and cone and between single and double cone opsin expression profiles, we calculated the relative proportion that each individual opsin gene contributed to the total pool of visual opsin genes expressed in a given species [as weighted species means based on TPM (transcripts per million)]. This proportion was calculated twice, once correcting the *RH2A*α/*RH2A*β proportion to account for the high degree of exonic sequence identity between these genes (Fig. 2 and table S3) and once without such a correction, leading to very similar results (fig. S4). Overall, very little variation in visual opsin gene expression profiles was found between specimens of the same species (barplots at the individual level are available on Dryad: https://datadryad.org/stash/dataset/doi:10.5061/dryad.r2280gbj2). Between species, however, our analyses revealed substantial differences with respect to the relative amount of rod versus cone opsin expression, and the number and relative proportion of visual opsin genes expressed in single and double cones (Fig. 2, figs. S4 and S5, and table S5): In all but two Eretmodini species (*Tanganicodus irsacae* and *Spathodus erythrodon*), the rod opsin (*RH1*) contributed to more than half of the total opsin expression in the retina (minimum, 42.90%; median, 82.55%; mean, 81.91%; maximum, 98.05%). The species expressing *RH1* the most (>90%) belonged mainly to the tribes Bathybatini, Boulengerochromini, Ectodini, and Trematocarini, which mostly occur at intermediate to greater water depths. Among the cone opsins, we found that double cone opsins

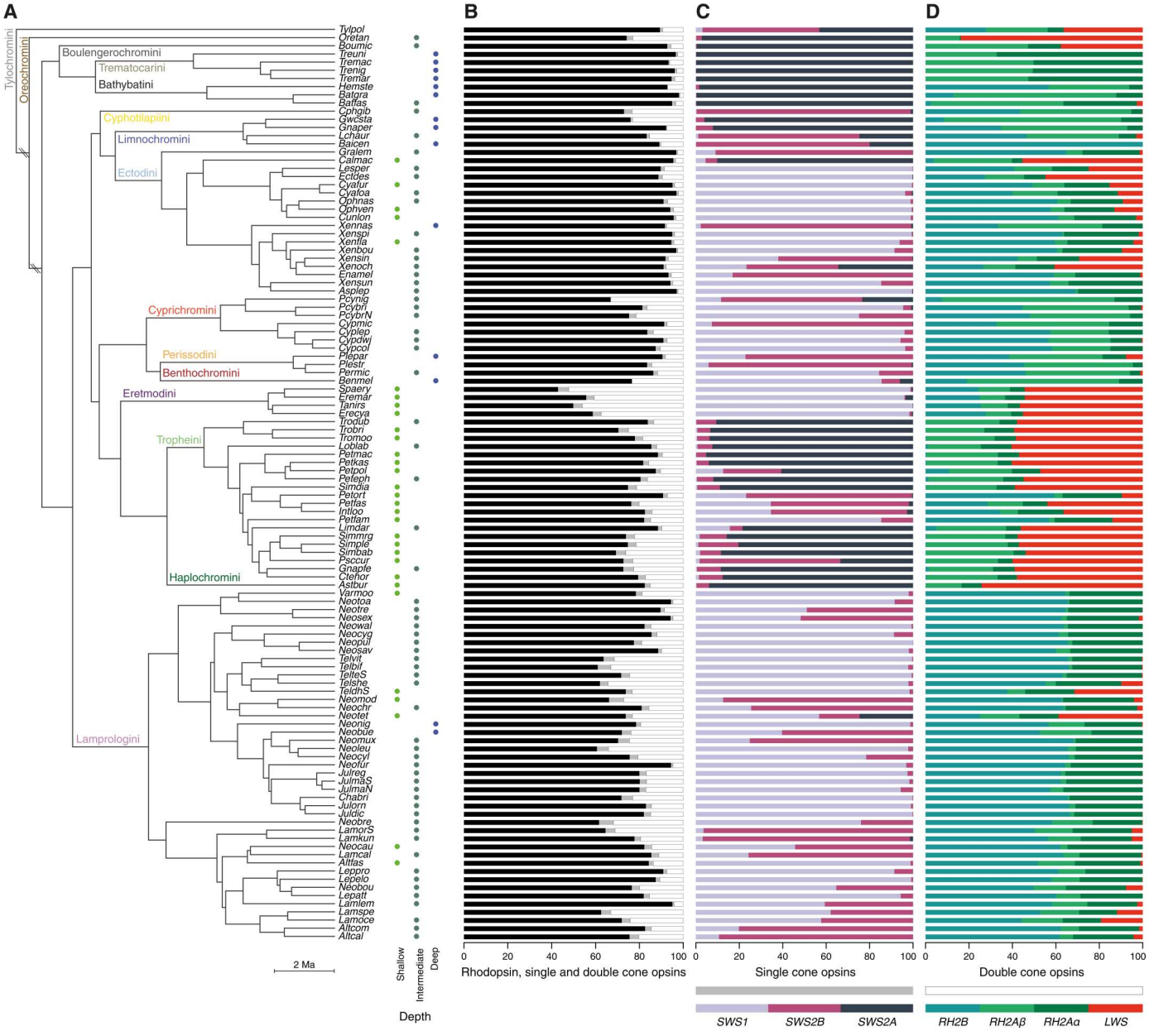

Fig. 2. Visual opsin gene expression profiles along the species tree of Lake Tanganyika cichlids. (**A**) Time-calibrated species tree of the cichlid fishes of Lake Tanganyika [taken from (*52*)], pruned to the focal taxa of this study (see table S1 for full species names, branches indicated with "\\" are not drawn to scale). For each species, the depth of occurrence—in three depth categories—is indicated and color-coded (absence of a dot indicates that the depth of occurrence is unknown for the species in question, or that the three depth categories do not adequately capture the ecology of a given species). (**B**) Relative proportions of rhodopsin versus cone opsin expression per species. (**C**) Relative proportions of single cone opsin expression per species. (**D**) Relative proportions of double cone opsin expression per species. Cone opsins are color-coded according to their spectral sensitivity. Single cone opsins include the UV-sensitive *SWS1*, the violet-sensitive *SWS2B*, and the blue-sensitive *SWS2A*. Double cone opsins comprise the green-sensitive *RH2B*, *RH2Aα*, and *RH2Aβ*, as well as the red-sensitive *LWS*.

(minimum, 1.63%; median, 14.63%; mean, 15.62%; maximum, 52.27%) were, on average, expressed 6.7 times (median, 6.5) more than single cone opsins (minimum, 0.001%; median, 2.42%; mean, 2.47%; maximum, 6.67%). This number comes close to the ratio of single to double cone photoreceptor cells previously reported for cichlid retinas [retinal mosaic of 1:4; (*10*, *68*), but see (*36*)]. However, high-resolution retinal images [e.g., fluorescent in situ hybridization of the retina (*69*)] would be required to confirm that the proportion of expressed single and double cone opsins reflects the number of single and double cone photoreceptor cells. The majority of species expressed predominantly one of the three single cone opsin genes (≥80% *SWS1* expression, N = 47 species; ≥80% *SWS2A*, N = 26; ≥80% *SWS2B*, N = 11), and typically two double cone opsins were expressed to a much greater extent [≥80% *RH2B* + *RH2As*, N = 78; ≥80% *RH2As* + *LWS*, N = 21; ≥80% *RH2B* + *LWS*, N = 2; note that for analytical reasons and just like in previous studies

(*47*, *48*, *56*), *RH2Aα* and *RH2Aβ* were combined here and denoted as *RH2As*]. *Paracyprichromis nigripinnis* (Cyprichromini) and *Benthochromis melanoides* (Benthochromini) were the only two species with close to zero single cone opsin expression (TPM of single cone opsins smaller than 2.5 for both species), and the four Trematocarini species as well as *Baileychromis centropomoides* (Limnochromini) were the only species with one cone opsin representing more than 99% of the double cone opsin expression (*RH2As* and *RH2B*, respectively).

To examine patterns of expression correlation among the visual opsin genes, we tested for pairwise (evolutionary) correlations of gene expression levels across the radiation [Spearman's *r* of TPMs and on phylogenetically independent contrasts (PICs) thereof; figs. S6 with *RH2As* and S7 with *RH2Aα* and *RH2Aβ*]. We detected numerous positive and negative correlations in gene expression levels across the visual opsin genes (out of 28 tests, 18 were significantly correlated based on TPMs and 15 based on PICs). For example, the expression of *SWS1* is positively correlated with that of *RH2B*, and the expression of *RH1* is negatively correlated with that of *RH2As* (fig. S6). We further observed that species tend to express a given opsin at the expense of one or more other opsins (e.g., *SWS1* versus *SWS2A* and *SWS2A* versus *RH2B*) and that this tendency is mainly driven by the distinct subset of expressed single cone opsin genes between species belonging to the tribes Bathybatini, Trematocarini, and Tropheini and the species of the remaining tribes (Fig. 2 and figs. S6 and S7).

Next, we used the cone opsin expression information to delineate visual palettes in cichlid fishes in Lake Tanganyika with two methods: (i) using the respective combinations of the most highly expressed single cone opsin and the two most highly expressed double cone opsins ("SDD majority-rule clustering") and (ii) using hierarchical clustering with a number of clusters (*k*) ranging from three to eight (fig. S8). Overall, our results revealed that most of the Tanganyikan cichlids express one of the three common visual palettes previously identified in cichlids (*31*, *47*, *56*, *70*), a short- (*SWS1* + *RH2B* + *RH2As*; present in 49 species with the SDD majority-rule clustering and in 50 species with $k = 3$ in the hierarchical clustering analysis), a middle- (*SWS2B* + *RH2B* + *RH2As*, 22 species with SDD; 34 species with $k = 3$), or a long-wavelength palette (*SWS2A* + *RH2As* + *LWS*, 18 species; 25 species with $k = 3$; Fig. 3 and figs. S8B and S9). When compared to previous findings (*47*), we were only able to reaffirm the visual palettes of 7 (using the hierarchical clustering with $k = 3$) out of 19 commonly studied species with our more sensitive detection method (RNA sequencing versus real-time quantitative polymerase chain reaction), our approximately twice as large sample size per species, and our exclusive use of specimens from the wild.

According to the SDD majority-rule clustering, there is evidence for the presence of five additional discrete visual palettes in Tanganyikan cichlids, including a shallow-water visual palette (*SWS1* + *RH2B* + *LWS*) that is exclusive to *Telmatochromis dhonti* (Lamprologini) and the four Eretmodini species investigated in our study, and a deep-water visual palette (*SWS2A* + *RH2B* + *RH2As*) exclusively expressed in eight species of the tribes Bathybatini, Limnochromini, and Trematocarini (Fig. 3 and fig. S8). Further, we found that the shallow- and deep-water visual palettes include three combinations of most highly expressed genes each (based on the majority-rule clustering of the complete set of single and double cone opsins; fig. S10). In addition, six other such combinations were depth-specific (*SWS2B* + *RH2B* + *RH2As*, two; *SWS2B* + *RH2B* + *LWS*, two; *SWS2A* + *RH2As* + *LWS*, two; fig. S10). The eight putative visual palettes suggested by the SDD majority-rule clustering are supported by a PCA based on the expression information of the cone opsin genes, which separated the different palettes, in particular along PC1 and PC3 (Fig. 3B and fig. S11, A to C). Future research, for example, using high-resolution imaging or single-cell gene expression information, would be necessary to validate the visual palettes.

We then performed ancestral state reconstructions on the basis of the visual palettes defined in this study and the time-calibrated species tree [taken from (*52*)] to investigate and compare turnovers between visual palettes. This was done once with the eight visual palettes identified with the SDD clustering (Fig. 3C) and once using the three visual palettes identified with the hierarchical clustering at $k = 3$ (fig. S9C). We found that at least three (when considering a total of eight visual palettes; Fig. 3, A and C) to five (when considering three visual palettes; fig. S9, A and C) transitions from another state to the short-wavelength palette occurred in the course of the cichlid radiation in Lake Tanganyika. According to these analyses, the long-wavelength visual palette emerged at least four times (Fig. 3, A and C, and fig. S9, A and C). The middle-wavelength palette arose at least 16 to 17 times, and from the short-wavelength palette in all but one case with the SDD clustering (in the Tropheini clade: *Petrochromis orthognathus*) and three cases with the hierarchical clustering at $k = 3$ (in the Tropheini clade: *P. polyodon*; *P. orthognathus*, *P. fasciolatus*, and *I. loocki*, and *Pseudosimochromis curvifrons*) (Fig. 3, A and C, and fig. S9, A and C). The shallow- and deep-water palettes are likely to have evolved twice each (Fig. 3C). An ancestral state reconstruction (phylomorphospace) based on a PCA of the expression information of the cone opsin genes and the species tree (*52*) supported the repeated evolution of the visual palettes within different clades (fig. S11, D to F), most clearly visible when PC1 and PC3 are compared (fig. S11E).

Ecological and morphological correlates of visual opsin gene expression

To test whether, at the macroevolutionary scale of an adaptive radiation, there is an association between the expression of visual opsin genes and ecological and morphological parameters, we performed linear regression (lm) and phylogenetic generalized least squares (pGLS) analyses, using available ecological and morphological data from the different Tanganyikan cichlid species and the time-calibrated species tree (*52*). Specifically, we tested for an association between individual visual opsin gene expression profiles and the stable carbon (C) and nitrogen (N) isotope composition as approximations for the relative position of a species along the benthic(littoral)–(deep)pelagic (from therein benthic-pelagic) macrohabitat axis ($\delta^{13}C$ value) (fig. S12) and the relative trophic level ($\delta^{15}N$ value) (fig. S13), respectively, as well as the relative eye size (fig. S14) as a putatively adaptive morphological trait in the context of vision [eye size data were extracted from morphometric analyses based on x-ray images from (*52*)]. In addition, to account for the multicollinearity of the expression profiles (see figs. S6 and S7), we fitted a phylogenetic partial least square regression (pPLS) for each of the eco/morphological proxies with all cone opsin expression profiles together. Our results showed that the expression of *RH2As* is positively associated with the benthic-pelagic trajectory ($\delta^{13}C$; see Fig. 4A for the pPLS analysis; pGLS: $R^2 = 0.084$, $P =$

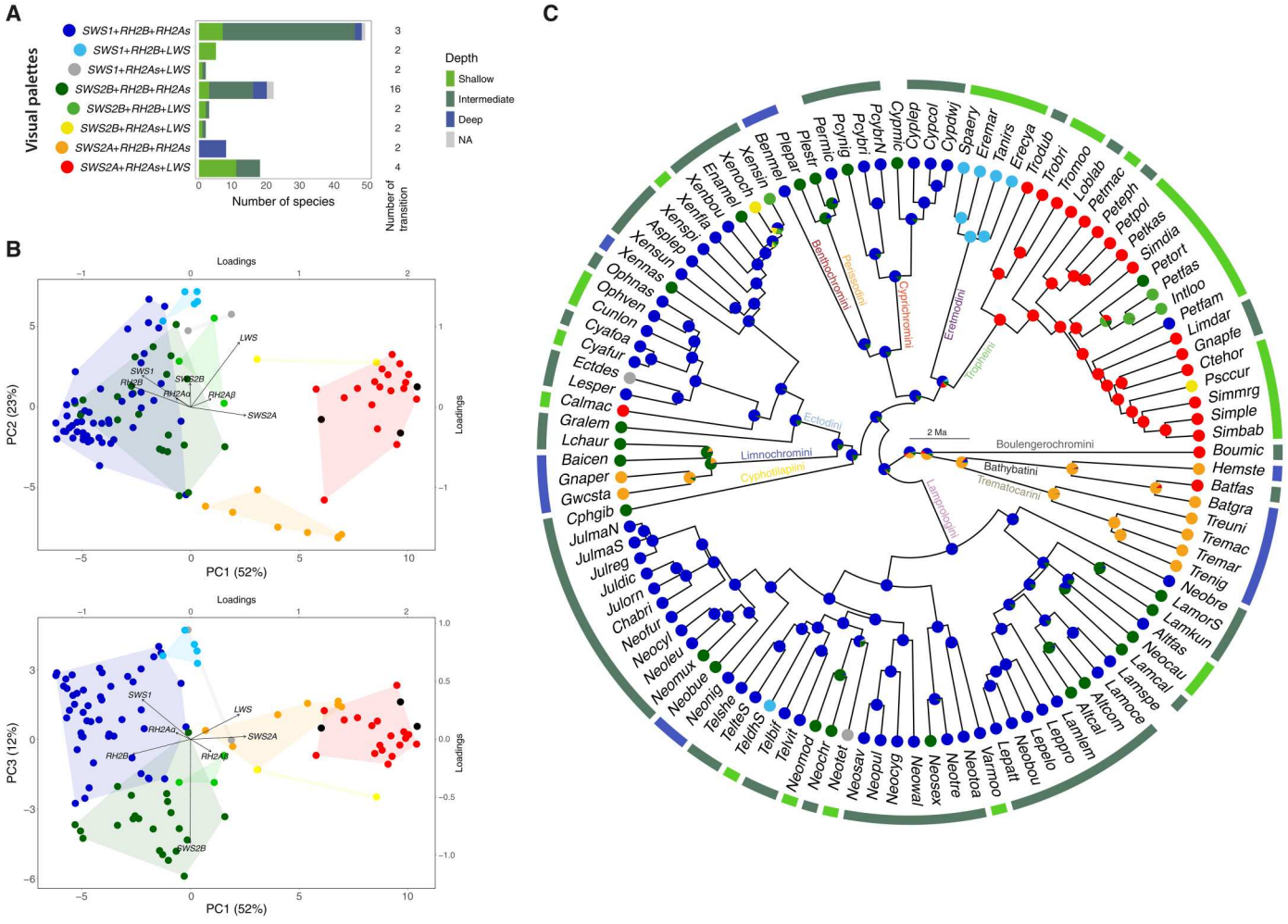

Fig. 3. Visual palette evolution in Lake Tanganyika cichlid fishes. (**A**) Barplot showing the number of species sharing one of the eight visual palettes identified based on the species-specific combinations of the most highly expressed single cone opsin and the two most highly expressed double cone opsins (SDD majority-rule clustering). Barplots are color-coded according to the respective proportion of species in the three depth categories at which the species occur. The number of evolutionary transitions into the respective visual palette according the ancestral state reconstruction shown in (C) is indicated on the right margin. (**B**) PCAs of the visual cone opsin gene expression levels. Each dot represents the weighted mean value of a given species and is color-coded according to the visual palettes defined in (A). The range of the visual palettes across the PCAs is indicated with convex hulls (except for *A. burtoni*, *O. tanganicae*, and *T. polylepis*). The loadings for PC1 and PC2 are represented with a black arrow. The variance explained by each principal component (PC) is reported in parenthesis. (**C**) Ancestral state reconstruction of visual palettes along the time-calibrated species tree [taken from (*52*) and pruned to the species included in this study (see table S1 for full species names]. Pie charts at the internal nodes indicate the relative posterior probability that the ancestor expressed each of the eight visual palettes and are color-coded according to the visual palettes shown in (A). Note that, just like in previous studies (*47*, *48*, *56*), *RH2A*α and *RH2A*β were combined under the category *RH2As*, and that the primarily riverine haplochromine *A. burtoni* as well as the more distantly related species *O. tanganicae* and *T. polylepis* were excluded from this analysis.

0.0022, λ = 0.85, fig. S12). Hence, species living in more shallow-water habitats express proportionally less *RH2As*, whereas species living in more pelagic and/or more deeper-water habitats express more *RH2As*. Further, we found that the negatively correlated single cone opsins *SWS1* and *SWS2A* (see Fig. 1C and fig. S6) are associated with the feeding ecology of the species (δ^{15}N; see Fig. 4B for the pPLS and fig. S13 for the pGLS analyses). More specifically, *SWS1* is proportionally overexpressed at lower trophic levels (pGLS: $R^2 = 0.09$, $P = 0.0014$, λ = 0.99; fig. S13) and *SWS2A* is proportionally overexpressed at higher trophic levels (pGLS: $R^2 = 0.09$, $P = 0.0015$, λ = 1; fig. S13). Last, our analyses uncovered a positive association between *RH1* expression and relative eye size (see Fig. 4C and fig. S14; pGLS: $R^2 = 0.09$, $P = 0.0015$, λ = 0.76).

DISCUSSION

The fine-tuning of the visual sensory system to better match the ambient light conditions is essential for the survival of many animal species and can be achieved through a number of molecular mechanisms including the duplication, functional diversification, and differential expression of visual opsin genes (*6*, *7*, *10*, *32*). In the present study, we report the sequencing and in-depth examination of 753 retinal transcriptomes from 112 endemic species of cichlid fishes from Lake Tanganyika with the aim to provide an understanding of (visual opsin) gene expression evolution in the macro-evolutionary context of a massive adaptive radiation.

At the whole retinal transcriptome level—that is, all protein-coding RNAs and lncRNAs combined, but also when protein-

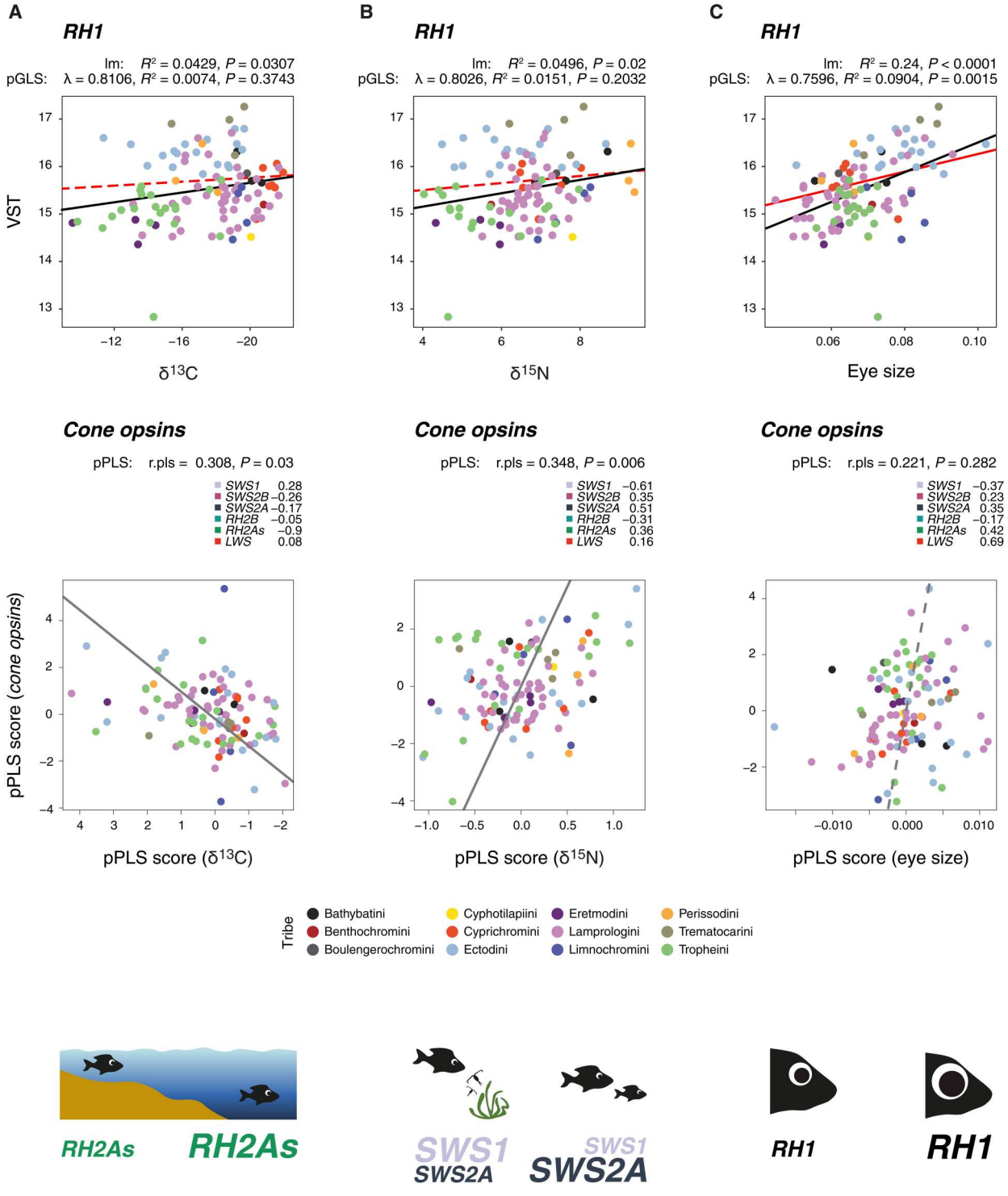

Fig. 4. Visual opsin gene expression and its association with macrohabitat, feeding ecology, and eye size. lm, pGLS, and pPLS analyses showing the associations between visual opsin gene expression (VST-normalized count) and (**A**) $\delta^{13}C$ values as habitat proxy for a species' position along the benthic-pelagic axis, (**B**) $\delta^{15}N$ values as proxy for the relative trophic level of a species, and (**C**) relative eye size. The top three panels show the association of rhodopsin (*RH1*) with the respective traits. The lm-fit is depicted in black, and the pGLS-fit is depicted in red (at $P < 0.05$ with a solid line). For each test, the *P* value (*P*) and the R-squared (R^2) are indicated, as well as the parameter lambda (λ) for the pGLS. The bottom three panels show scatter plots of the pPLS of the cone opsins and the ecological and morphological traits. The pPLS-fit is depicted as a gray line (at $P < 0.05$ with a solid line). The corresponding pPLS coefficient (r-PLS) and the *P* value (*P*) along with the PLS loadings are indicated above each plot. Each dot represents a species and is color-coded according to tribe. The tests for an association of individual cone opsin expression level and each ecological/morphological trait are provided in the Supplementary Materials as figs. S12 to S14. The primarily riverine haplochromine *A. burtoni* as well as the more distantly related species *O. tanganicae* and *T. polylepis* were excluded from this analysis.

coding features and lncRNAs are considered individually (Fig. 1 and fig. S3)—our results confirm the general trend in vertebrates (*71*), including in cichlids (*59*), that the transcriptome-wide patterns of gene expression differentiation in a given tissue mirror phylogeny. However, unlike in the other tissues that have been investigated in such a detail and with a similar taxonomic coverage across the adaptive radiation of cichlid fishes in Lake Tanganyika (brain, gills, liver, ovary/testis, and lower pharyngeal jaw bone) (*59*), there is no such clear separation in global gene expression patterns in retinal tissue between the Lamprologini—the most species-rich cichlid tribe in Lake Tanganyika—and the rest of the radiation.

In aquatic ecosystems of sufficient depth, the light environment changes most along the depth gradient, which is due to the optical properties of water (*27*, *28*). While a water depth–related pattern is not apparent from the PCA of overall gene expression levels in the cichlid assemblage of Lake Tanganyika (Fig. 1A), there is an obvious separation between shallow- and deep-water living species when only the top 100 (Fig. 1B) or the top 500 genes (fig. S3C) with the greatest variance in our dataset, or only the visual opsin genes (Fig. 1C), are considered. All seven cone opsins rank among the top 100 most differentially expressed genes in the retina, with *LWS* being the single-most differentially expressed gene overall and all cone opsin genes ranking in the top 37 genes (table S4). In addition to the cone opsins, we also found 14 other vision-related genes, plus 5 genes with a known function in circadian rhythm regulation, and 8 hemoglobin subunit genes (likely expressed in the retinal vasculature) among top 100 most differentially expressed genes. Together, this suggests that in cichlids from Lake Tanganyika, gene-regulatory processes may have played a crucial role in the repeated (Fig. 3) and rapid (in less than 10 million years) adaptations of the retina to deep-water conditions characterized by light of a narrower spectral waveband and reduced levels of dissolved oxygen.

In contrast to the cone opsins that mediate color discrimination, the rod opsin (*RH1*) responsible for scotopic vision is not in the top 100 most differentially expressed retinal genes across the Tanganyikan cichlid fauna (it ranks at position 849). *RH1* is by far the most highly expressed visual opsin gene in Tanganyikan cichlids (>50% of the total visual opsin expression levels in all species except for two Eretmodini representatives; median, 82.55%; mean, 81.91%; Fig. 2 and table S5), which is most likely due to the comparatively larger number of rod photoreceptor cells compared to cones in the cichlid retina (*10*, *68*). We also found that *RH1* expression levels are associated with relative eye size (Fig. 4C), suggesting that bigger eyes either contain proportionally more rods expressing *RH1* at similar levels as in smaller eyes or contain rods that express proportionally more *RH1*. In any case, relative *RH1* expression levels do not significantly scale with our proxy for the benthic-pelagic axis (the stable carbon isotope signature; Fig. 4A), nor is there an obvious association with species-specific water depth categories (Fig. 2 and fig. S5). Instead, it has previously been shown that specific amino acid substitutions in *RH1*, often at so-called key tuning sites, correlate strongly with water depth in cichlids from lakes Malawi and Tanganyika (*30*, *72*, *73*). This suggests that the fine-tuning of scotopic vision along the depth gradient—for which in Tanganyikan cichlids (*30*), just as in most other vertebrate species (*14*, *21*), only one single opsin (*RH1*) is responsible—is primarily achieved via adaptive modifications of the *RH1* coding sequence, whereas the fine-tuning of photopic vision, which involves up to seven cone opsin genes in cichlids (*47*, *48*), seems to involve changes in their expression levels. Future studies should examine the cone opsin coding sequences in more detail in Lake Tanganyika cichlids, also with respect to adaptive changes at putative key tuning sites.

Overall, we found that all studied cichlid species from Lake Tanganyika expressed *RH1* as well as the cone opsins *SWS2B*, *RH2B*, *RH2A*α, and *RH2A*β (Fig. 2 and table S5), which cover, together with *SWS2A*, the central waveband of the visible light spectrum. On the other hand, six species did not express *SWS1* (Bathybatini: *Bathybates fasciatus*, *Hemibates stenosoma*; Boulengerochromini: *Boulengerochromis microlepis*; Limnochromini: *Gnathochromis permaxillaris*, *Limnochromis staneri*; Trematocarini: *Trematocara nigrifrons*), of which only *B. microlepis* is not strictly living in deeper waters and *T. nigrifrons* lives in the depth and migrates during the night into shallower zone of the lake; for three species living at intermediate water depths, we did not find an expression signal for *SWS2A* (Ectodini: *Lestradea perspicax*, *Xenotilapia boulengeri*; Lamprologini: *Neolamprologus savoryi*), and four species had no *LWS* expression (Bathybatini: *H. stenosoma*; Lamprologini: *Neolamprologus pulcher*; Limnochromini: *G. permaxillaris*; Trematocarini: *Trematocara macrostoma*), which are all deep-water species except for *N. pulcher* living at intermediate depths. Two deep-water species (*G. permaxillaris* and *H. stenosoma*) thus lack expression of both the shortest- (*SWS1*) and the longest-wavelength sensitive (*LWS*) cone opsins. In one intermediate- and two deep-water species, we could further attribute the lack of expression to the pseudogenization of a particular cone opsin gene (*SWS2A* in *X. boulengeri*; *SWS1* in *T. nigrifrons*; *LWS* in *T. macrostoma*), suggesting that these species have transitioned from zero expression ("non-usage") of a cone opsin gene, as observed in a number of primarily deep-water living cichlid species in Lake Tanganyika (see above), to cone opsin loss ("degeneration"), as seen in many marine fish living at greater water depths (*23*, *25*).

A second major axis of expression differentiation in visual opsin genes in fishes occurs in response to differences in feeding ecology (*10*). By and large, we confirm previous results in Lake Malawi cichlids, where expression levels of the UV-sensitive *SWS1* correlate with food type, and algae and plankton eaters feature higher *SWS1* expression levels possibly enhancing UV vision (*47*, *48*, *74*, *75*). In our analysis of 112 Tanganyikan cichlid species, we found that *SWS1* shows a significant association with our proxy for trophic ecology, the stable nitrogen isotope signature, but we also found that *SWS2A* is associated with feeding ecology (Fig. 4B), with species at lower trophic levels expressing proportionally more *SWS1* and less *SWS2A*, and vice versa. Cichlid species at the lower end of the trophic chain (algae and plankton eaters) express more *SWS1*, confirming the increase of UV sensitivity to better detect the UV-absorbing zooplankton against a bright UV background (*47*, *48*, *75*). On the other hand, algae- and plankton-eating species express less *SWS2A*. Species express either *SWS1* or *SWS2A* (Fig. 4 and figs. S5 to S7), suggesting that these two single cone opsin genes might have a similar function (better detection of feeding items against the background).

In African cichlid fishes, visual opsin gene expression is typically categorized in the form of visual palettes, defined by the dominating single and the two most highly expressed double cone opsins (*31*, *36*, *47*, *48*, *56*). Three main visual palettes have so far been identified in cichlids: a short- (dominated by *SWS1* + *RH2B* + *RH2As*), a middle- (*SWS2B* + *RH2B* + *RH2As*), and a long-wavelength visual

palette (*SWS2A* + *RH2As* + *LWS*). In the present study, we confirm that most cichlid species from Lake Tanganyika express one of these three visual palettes (Fig. 3 and figs. S8 and S9). However, we provide evidence for at least two additional visual palettes that are associated with a particular light environment: (i) a visual palette dominated by the cone opsins having their peak spectral sensitivities at both ends of the visible light spectrum (*SWS1* + *RH2B* + *LWS*) characteristic of one Lamprologini and four Eretmodini species, which are all among the most shallow-water living cichlid species that occur in Lake Tanganyika, and (ii) a visual palette dominated by the cone opsins sensitive to the most central waveband of the spectrum (*SWS2A* + *RH2B* + *RH2As*) exclusive to deep-water living species of the tribes Bathybatini, Limnochromini, and Trematocarini (Fig. 3). Our ancestral state reconstruction of visual palettes along the time-calibrated species tree showed that numerous evolutionary transitions occurred between visual palettes in the course of the adaptive radiation of cichlid fishes in Lake Tanganyika (Fig. 3C and fig. S9C). The visual sensory system thus emerges as yet another highly dynamic trait complex in Lake Tanganyika cichlids, in addition to body shape (*52*), trophic morphology (*52*, *76*), body pigmentation (*52*), and sex determination systems (*77*).

Overall, we found that, at the macroevolutionary and ecosystem level of a massive adaptive radiation of cichlid fishes, changes in the expression of core components of the visual sensory system, the visual opsin genes, play a major role in visual adaptation. Through the examination of 753 retinal expression profiles in 112 closely related cichlid species from Lake Tanganyika, we identified three main axes of visual system tuning: (i) The visual system of shallow-water and more benthic cichlid species is characterized by proportionally lower expression levels of the green-sensitive *RH2A*s, whereas deeper living and more pelagic species express more *RH2A*s (Fig. 4A); (ii) cichlid species at the lower end of the trophic chain (algae and plankton eaters) express proportionally more of the UV-sensitive *SWS1* and less of the blue-sensitive *SWS2A*, whereas the opposite is true for more predatorial cichlids including the scale-eaters of the tribe Perissodini (Fig. 4B); and (iii) species with larger eyes express proportionally more *RH1* and vice versa (Fig. 4C). This suggests that, when the entire adaptive radiation of cichlid fishes in Lake Tanganyika is considered, adaptations to a particular light environment involve a trade-off in the relative levels of visual opsin gene expression between a subset of cone opsin genes [*RH2As* along the depth gradient, *SWS1* and *SWS2A* along the trophic level; Fig. 4]. Together, our in-depth examination of hundreds of retinal transcriptomes sheds light on the dynamics and the changes in the expression of visual opsin genes in the adaptive radiation of cichlid fishes in Lake Tanganyika.

MATERIALS AND METHODS

Experimental design

In this study, we sequenced 753 new retinal transcriptomes of 112 cichlid species from African Lake Tanganyika to (i) identify adaptive changes in the expression of rod and cone visual opsin genes, (ii) define and reconstruct the evolution of visual palettes on the basis of cone opsin expression levels, and (iii) examine rod and cone opsin expression levels in relation to macrohabitat, diet, and relative eye size.

Sampling and dataset

Sampling of fish eyes was performed between 2014 and 2020 at 44 locations at Lake Tanganyika covering the entire north-south axis of this approximately 670-km-long lake. Sampling and sample exportation were performed in accordance to the relevant permits issued by the (i) Ministère de l'Eau, de l'Environnement, de l'Aménagement du Territoire et de l'Urbanisme, Republic of Burundi (nr. 770 06/62710), the Université du Burundi (Cabinet du Recteur and Directeur de la Recherche et de l'Innovation; nr. 2014/R991), and the Permanent Mission of the Republic of Burundi to the United Nations, Geneva (work permits 544-547/GE/2014), for the Republic of Burundi; (ii) the Tanzania Commission for Science and Technology (COSTECH; research permits 2015-176-NA-2015 and 2016-373-NA-2015-96), the Tanzania National Parks Authority (TANAPA; research permits TNP/HQ/C.10/13/2015 and TNP/HQ/C.10/13/2017), the Tanzania Wildlife Research Institute (TAWIRI; permit 13300), the Department of Immigration (permits CTA0329016 and RPC11100834), and the Tanzanian Fisheries Research Institute (TAFIRI; permits TAF/KGM/R/VOL.V/236 and TAF/KGM/R.1/VOL.V/121) for the United Republic of Tanzania; and (iii) the Department of Immigration (study permits SP000627, SP001995, SP004273, SP005937, and SP226456) and the Department of Fisheries for the Republic of Zambia. Sampling and all further experiments were approved by the appropriate ethics committees.

Fish were caught with barrier nets while snorkeling or scuba diving or purchased from local fishermen, covering a depth range of <1 to >100 m (note that in Lake Tanganyika fish occur down to the oxycline at 150 to 200 m). Eyes were dissected in the field from freshly caught specimens after the fish had been euthanized and photographed, measured, and weighted. Both eyes from a given specimen were stored in RNAlater (Ambion) until further steps in the laboratory (see below). Our final dataset included eyes of 753 adult specimens, representing at least three male and three female individuals of 112 species covering all 12 Tanganyikan cichlid tribes (Bathybatini, Benthochromini, Boulengerochromini, Cyphotilapiini, Cyprichromini, Ectodini, Eretmodini, Lamprologini, Limnochromini, Perissodini, Trematocarini, and Tropheini) and one representative each of the tribes Haplochromini, Oreochromini, and Tylochromini (see table S1 for details on samples, sampling dates and localities, and sex).

The following additional data from our previous work were included in this study: The time-calibrated species tree based on genome-wide data, raw sequencing data [National Center for Biotechnology Information (NCBI) BioProject accession no. PRJNA550295], gene duplication and positive selection analyses, stable carbon (C) and nitrogen (N) isotope signatures, and relative eye size data were taken from Ronco *et al.* (*52*) (data available on Dryad: https://datadryad.org/stash/dataset/doi:10.5061/dryad.9w0vt4bbf), and habitat categories (shallow water depth of 0 to 10 m, intermediate water depth of 10 to 20 m, and deep water depth of >20 m) were taken from Ricci *et al.* (*30*) (data available on Dryad: https://datadryad.org/stash/dataset/doi:10.5061/dryad.4mw6m90c7).

Dissection, extraction, library preparation, and Illumina sequencing

For each specimen, the retina of a single eye was dissected and homogenized (FastPrep-24; MP Biomedicals), and the total RNA was

extracted using the Direct-zol RNA kit (Zymo) according to the manufacturer's protocol. Individual libraries were constructed using the Illumina TruSeq stranded protocol including RiboZero Gold rRNA depletion (Illumina) and sequenced on Illumina NovaSeq 6000 in PE 100-bp mode. Library construction and sequencing were conducted at the Genomics Facility Basel, which is jointly operated by the University of Basel and the Department of Biosystems Science and Engineering (D-BSSE) of ETH Zurich. Samples were randomized with respect to species and sex for both the dissection/extraction and the sequencing steps. Library preparations of 84 samples failed in a first attempt but could successfully be repeated in a second round. If two sequencing runs were performed for a given sample, the runs were combined for downstream analyses. The raw read data from all 753 samples are available from NCBI under the BioProject accession number PRJNA913112.

Quality filtering, mapping, and read counting

Quality filtering and adapter removal of Illumina strand-specific paired-end sequences were performed using Trimmomatic [v. 0.39; (*78*)] with a 4-bp window size, a required window quality of 15, and 80 bp as minimum read length. As in our previous work (*59*), cleaned reads were mapped against the Nile tilapia reference genome (*O. niloticus*; RefSeq accession GCF_001858045.2, female), which is phylogenetically equidistant to all members of the cichlid adaptive radiation in Lake Tanganyika (that is, all species in our dataset except *O. tanganicae* and *T. polylepis*), using STAR [v. 2.7.3a; (*79*)] with --outFilterMultimapNmax 1 --outFilterMatchNminOverLread 0.4 --outFilterScoreMinOverLread 0.4. To obtain a reasonable estimate of mapped reads to exonic features, we filtered out mapped singletons and then assigned and counted read pairs within exons using the HTSeq-count script from the HTSeq framework [v. 0.11.2; (*80*)]. Because of the high gene sequence similarity between *RH2A*α and *RH2A*β (percent sequence identity of exons between 94.81 and 99.40%; table S5), we retrieved all read pairs exactly mapping to both features and corrected the read count by assigning the remaining read pairs to *RH2A*α and *RH2A*β according to their original ratio. The total number of exonic features retrieved by HTSeq-count was 41,945 (out of 42,622 annotated genes; see data S1). We filtered the read count dataset to retain both protein-coding RNAs and lncRNAs (*59*, *81*). This resulted in 38,228 RNAs, from which we excluded 9226 lowly expressed genes (≤5 counts in less than three samples). The final read count dataset used for the subsequent analyses included 29,002 RNAs, from which 25,335 were protein-coding RNAs (out of 29,532 exonic feature) and 3667 were lncRNAs (out of 8696 exonic features).

Principal components analysis

Before PCA, we normalized the final read count dataset using the R package DESeq2 [v. 1.34.0; (*82*)]. We set the experimental design formula to "~ species + sex" and converted the data using VST [with parameter blind = FALSE; see (*59*)]. We then calculated the weighted species mean of VST values per gene to rely on samples with higher number of sequenced reads. PCAs were performed with the prcomb function in R (*83*) for the overall dataset containing both protein-coding RNAs and lncRNAs, for protein-coding RNAs and lncRNAs individually, for the top 500 and the top 100 genes with the greatest variance in gene expression, and for the visual opsin genes. In addition, we performed a PCA based on the expression information of the cone opsin genes to validate the visual palettes delineated using the clustering methods (see below) and reconstructed ancestral states along the time-calibrated species of (*52*) with the phylomorphospace function of the R package phytools (v. 0.7-90) (*84*).

Opsin expression profiles and visual palette identification

To account for variation in sequencing depth and visual opsin gene length, we converted the final read count dataset to TPM and calculated the weighted species means of TPM per gene to rely on samples with higher numbers of sequenced reads. We then calculated the percent of weighted species mean TPM of each visual opsin gene relative to the total visual opsin pool and to opsin categories (single cone opsins: *SWS1*, *SWS2B*, and *SWS2A*; double cone opsins: *RH2B*, *RH2A*α, *RH2A*β, and *LWS*; in addition to the rhodopsin *RH1* and cone opsins).

To examine the pattern of expression correlation of visual opsin genes, we tested for correlations (Spearman's correlation coefficients) between all pairs of opsins using the percent weighted species mean TPM of each visual opsin gene relative to the total visual opsin pool. We further calculated PICs [pic function of the R package ape; v. 5.5; (*85*)] along the species tree and inferred Spearman's correlation coefficients for PICs (i.e., through the origin) using the cor.table function of the R package picante [v. 1.8.1, (*86*)]. *P* values were adjusted for multiple testing using the Benjamini and Hochberg method.

To characterize visual palettes in the cichlid fish fauna of Lake Tanganyika, we applied two strategies: (i) defining visual palettes according to the single-most highly expressed single cone opsin and the two most highly expressed double cone opsins applying a majority-rule criterion (SDD majority-rule clustering) and (ii) performing a hierarchical clustering analysis with the number of clusters (*k*) ranging from three to eight and using the R function hclust with the Ward's method [see (*48*)], cross-validated with the *k*-nearest neighbor (knn) classification method. We opted for the SDD majority-rule clustering method to account for the predominant expression level (≥80%) of a unique single cone opsin and two double cone opsins and confirmed our findings by applying the majority-rule clustering method on the complete set of single and double cone opsins. For these analyses, we combined *RH2A*α and *RH2A*β into the category *RH2As*, as it has been done in previous studies (*48*, *54*, *56*, *87*), and we also included species with close to zero cone opsin expression or with a predominant expression of one double cone opsin. For the SDD majority-rule and the hierarchical clustering methods, we then reconstructed the ancestral states of visual palettes along the species tree using make.simmap function of the R package phytools (*84*) [with 10,000 simulations, an equal-rates model, the maximum likelihood method, and a Bayesian Markov-Chain Monte-Carlo (MCMC) strategy]. As this part of our study focused exclusively on the adaptive radiation of cichlid fishes in Lake Tanganyika as defined in (*52*), we excluded the primarily riverine haplochromine species *A. burtoni* (Haplochromini) and the two distantly related species of the tribes Oreochromini and Tylochromini.

Regression analyses

We then examined whether, at the level of the entire adaptive radiation, there is an association between visual opsin gene expression levels and ecological and morphological traits. Using lm and pGLS

analyses [pgls function of the R package caper; v. 1.0.1; (*88*)], we thus analyzed the relationship between weighted species mean VST-normalized count of visual opsins and (i) $\delta^{13}C$ values as macrohabitat proxy, (ii) $\delta^{15}N$ values as proxy for relative trophic level, and (iii) relative eye size (as ratio of square root of the eye area and centroid size). Furthermore, to account for the multicollinearity of the expression profiles (see figs. S6 and S7), we fitted a pPLS for each of the eco/morphological traits and all cone opsin expression profiles [phylo.integration function of the R package geomorph; v. 4.0.4; (*89*)]. Again, we combined *RH2A*α and *RH2A*β into *RH2As*. For the same reasons as mentioned above, we again excluded the single representatives each of Haplochromini, Oreochromini, and Tylochromini. Last, to highlight the relationships among the ecological and morphological traits, we performed lm and pGLS analyses between the species' $\delta^{13}C$ values, $\delta^{15}N$ values, and relative eye size (fig. S15A), plus a phylogenetic analysis of variance (ANOVA) between the species' depth of occurrence and each ecological and morphological trait (fig. S15B and table S6) using the phylANOVA function of the R package phytools (*84*) (with 1000 simulations and "BH" as method).

Genomic analyses

To screen for possible duplications of particular visual opsin genes in Tanganyikan cichlids, we reinspected the gene duplication estimates of 488 genomes (246 taxa) from Ronco *et al.* (*52*). Furthermore, we used the cichlid-tailored opsin raw read mapping approach of Ricci *et al.* (*30*) to confirm the presence of a single copy per cone opsin gene [*RH1* results in (*30*)] and to retrieve the protein-coding sequences in 517 genomes (271 species, including outgroups and nonendemic species nested in the radiation). We further examined the completeness of the protein-coding sequence of the visual opsins with no gene expression. Last, we reinspected signals of positive selection in the cone opsin genes [no data available for *RH2A*α and *RH2A*β; *RH1* results in (*30*)] by extracting the d_N/d_S ratio per opsin in 471 genomes (243 taxa) from the positive selection analysis of (*52*). Note that we did not test for positive selection across sites [see (*58*)] but instead used the available data of (*52*).

Statistical analysis

All statistical tests and parameters are reported in Materials and Methods and in the figure legends. Statistical analyses were performed using R (v. 4.1.2 and 4.2.2).

Supplementary Materials

This PDF file includes:
Figs. S1 to S15
Tables S1 to S6
Legend for data S1

Other Supplementary Material for this manuscript includes the following:
Data S1

REFERENCES AND NOTES

1. A. J. Hudspeth, N. K. Logothetis, Sensory systems. *Curr. Opin. Neurobiol.* **10**, 631–641 (2000).
2. M. F. Land, Biology of sensory systems. *Trends Neurosci.* **23**, 588–589 (2000).
3. T. J. Ness, T. J. Brennan, Sensory systems, in *Foundations of Anesthesia: Basic Sciences for Clinical Practice* (Elsevier, 2006), pp. 257–266.
4. D. M. Hunt, M. W. Hankins, S. P. Collin, N. J. Marshall, The evolution of photoreceptors and visual photopigments in vertebrates, in *Evolution of Visual and Non-Visual Pigments* (Springer-Verlag, 2014), pp. 163–217.
5. M. Inoue-Murayama, S. Kawamura, A. Weiss, *From Genes to Animal Behavior: Social Structures, Personalities, Communication by Color* (Springer, 2011).
6. P. Oteiza, M. W. Baldwin, Evolution of sensory systems. *Curr. Opin. Neurobiol.* **71**, 52–59 (2021).
7. M. W. Baldwin, M. C. Ko, Functional evolution of vertebrate sensory receptors. *Horm. Behav.* **124**, 104771 (2020).
8. T. W. Cronin, S. Johnsen, N. J. Marshall, E. J. Warrant, *Visual Ecology* (Princeton Univ. Press, 2014).
9. J. N. Lythgoe, *The Ecology of Vision* (Clarendon Press, 1979).
10. Z. Musilova, W. Salzburger, F. Cortesi, The visual opsin gene repertoires of teleost fishes: Evolution, ecology, and function. *Annu. Rev. Cell Dev. Biol.* **37**, 441–468 (2021).
11. M. F. Land, D.-E. Nilsson, Animal eyes. *Zool. J. Linn. Soc.* **166**, 912 (2012).
12. T. H. Oakley, D. I. Speiser, How complexity originates: The evolution of animal eyes. *Annu. Rev. Ecol. Evol. Syst.* **46**, 237–260 (2015).
13. M. F. Land, The optical structures of animal eyes. *Curr. Biol.* **15**, R319–R323 (2005).
14. J. K. Bowmaker, Evolution of vertebrate visual pigments. *Vision Res.* **48**, 2022–2041 (2008).
15. K. Palczewski, T. Kumasaka, T. Hori, C. A. Behnke, H. Motoshima, B. A. Fox, I. Le Trong, D. C. Teller, T. Okada, R. E. Stenkamp, M. Yamamoto, M. Miyano, Crystal structure of rhodopsin: A G protein-coupled receptor. *Science* **289**, 739–745 (2000).
16. G. Wald, The molecular basis of visual excitation. *Nature* **219**, 800–807 (1968).
17. D. C. Teller, R. E. Stenkamp, K. Palczewski, Evolutionary analysis of rhodopsin and cone pigments: Connecting the three-dimensional structure with spectral tuning and signal transfery. *FEBS Lett.* **555**, 151–159 (2003).
18. S. Yokoyama, Molecular evolution of vertebrate visual pigments. *Prog. Retin. Eye Res.* **19**, 385–419 (2000).
19. S. Yokoyama, Evolution of dim-light and color vision pigments. *Annu. Rev. Genomics Hum. Genet.* **9**, 259–282 (2008).
20. W. Wang, J. H. Geiger, B. Borhan, The photochemical determinants of color vision. *Bioessays* **36**, 65–74 (2014).
21. W. I. L. Davies, S. P. Collin, D. M. Hunt, Molecular ecology and adaptation of visual photopigments in craniates. *Mol. Ecol.* **21**, 3121–3158 (2012).
22. T. D. Lamb, S. P. Collin, N. P. J. Edward, Evolution of the vertebrate eye: Opsins, photoreceptors, retina and eye cup. *Nat. Rev. Neurosci.* **8**, 960–976 (2007).
23. Z. Musilova, F. Cortesi, M. Matschiner, W. I. L. Davies, J. S. Patel, S. M. Stieb, F. De Busserolles, M. Malmstrøm, O. K. Tørresen, C. J. Brown, J. K. Mountford, R. Hanel, D. L. Stenkamp, K. S. Jakobsen, K. L. Carleton, S. Jentoft, J. Marshall, W. Salzburger, Vision using multiple distinct rod opsins in deep-sea fishes. *Science* **364**, 588–592 (2019).
24. F. Cortesi, Z. Musilová, S. M. Stieb, N. S. Hart, U. E. Siebeck, M. Malmstrøm, O. K. Tørresen, S. Jentoft, K. L. Cheney, N. J. Marshall, K. L. Carleton, W. Salzburger, Ancestral duplications and highly dynamic opsin gene evolution in percomorph fishes. *Proc. Natl. Acad. Sci. U.S.A.* **112**, 1493–1498 (2015).
25. J. J. Lin, F. Y. Wang, W. H. Li, T. Y. Wang, The rises and falls of opsin genes in 59 ray-finned fish genomes and their implications for environmental adaptation. *Sci. Rep.* **7**, 15568 (2017).
26. J. T. O. Kirk, *Light and Photosynthesis in Aquatic Ecosystems* (Cambridge Univ. Press, 1983).
27. E. J. Warrant, N. A. Locket, Vision in the deep sea. *Biol. Rev. Camb. Philos. Soc.* **79**, 671–712 (2004).
28. F. W. Munz, W. N. McFarland, Evolutionary adaptations of fishes to the photic environment, in *The Visual System in Vertebrates*, F. Crescitelli, Ed. (Springer-Verlag, 1977), pp. 193–274.
29. S. Yokoyama, R. Yokoyama, Adaptive evolution of photoreceptors and visual pigments in vertebrates. *Annu. Rev. Ecol. Syst.* **27**, 543–567 (1996).
30. V. Ricci, F. Ronco, Z. Musilova, W. Salzburger, Molecular evolution and depth-related adaptations of rhodopsin in the adaptive radiation of cichlid fishes in Lake Tanganyika. *Mol. Ecol.* **31**, 2882–2897 (2022).
31. K. Carleton, Cichlid fish visual systems: Mechanisms of spectral tuning. *Integr. Zool.* **4**, 75–86 (2009).
32. K. L. Carleton, D. Escobar-Camacho, S. M. Stieb, F. Cortesi, N. J. Marshall, Seeing the rainbow: Mechanisms underlying spectral sensitivity in teleost fishes. *J. Exp. Biol.* **223**, jeb193334 (2020).
33. F. E. Hauser, B. S. Chang, Insights into visual pigment adaptation and diversity from model ecological and evolutionary systems. *Curr. Opin. Genet. Dev.* **47**, 110–120 (2017).
34. F. E. Hauser, K. L. Ilves, R. K. Schott, E. Alvi, H. López-Fernández, B. S. W. Chang, Evolution, inactivation and loss of short wavelength-sensitive opsin genes during the diversification of Neotropical cichlids. *Mol. Ecol.* **30**, 1688–1703 (2021).

35. N. J. Marshall, F. Cortesi, F. de Busserolles, U. E. Siebeck, K. L. Cheney, Colours and colour vision in reef fishes: Past, present and future research directions. *J. Fish Biol.* **95**, 5–38 (2019).
36. Z. Musilova, A. Indermaur, A. R. Bitja-Nyom, D. Omelchenko, M. Kłodawska, L. Albergati, K. Remišová, W. Salzburger, Evolution of the visual sensory system in cichlid fishes from crater lake Barombi Mbo in Cameroon. *Mol. Ecol.* **28**, 5010–5031 (2019).
37. R. K. Schott, S. P. Refvik, F. E. Hauser, H. López-Fernández, B. S. W. Chang, Divergent positive selection in rhodopsin from lake and riverine cichlid fishes. *Mol. Biol. Evol.* **31**, 1149–1165 (2014).
38. Y. Terai, R. Miyagi, M. Aibara, S. Mizoiri, H. Imai, T. Okitsu, A. Wada, S. Takahashi-Kariyazono, A. Sato, H. Tichy, H. D. J. Mrosso, S. I. Mzighani, N. Okada, Visual adaptation in Lake Victoria cichlid fishes: Depth-related variation of color and scotopic opsins in species from sand/mud bottoms. *BMC Evol. Biol.* **17**, 200 (2017).
39. K. L. Carleton, M. R. Yourick, Axes of visual adaptation in the ecologically diverse family Cichlidae. *Semin. Cell Dev. Biol.* **106**, 43–52 (2020).
40. F. de Busserolles, L. Fogg, F. Cortesi, J. Marshall, The exceptional diversity of visual adaptations in deep-sea teleost fishes. *Semin. Cell Dev. Biol.* **106**, 20–30 (2020).
41. W. R. A. Muntz, Yellow filters and the absorption of light by the visual pigments of some amazonian fishes. *Vision Res.* **13**, 2235–2254 (1973).
42. J. Torres-Dowdall, F. Henning, K. R. Elmer, A. Meyer, Ecological and lineage-specific factors drive the molecular evolution of rhodopsin in cichlid fishes. *Mol. Biol. Evol.* **32**, 2876–2882 (2015).
43. D. J. Rennison, G. L. Owens, J. S. Taylor, Opsin gene duplication and divergence in ray-finned fish. *Mol. Phylogenet. Evol.* **62**, 986–1008 (2012).
44. G. L. Owens, D. J. Rennison, Evolutionary ecology of opsin gene sequence, expression and repertoire. *Mol. Ecol.* **26**, 1207–1210 (2017).
45. C. J. Weadick, B. S. W. Chang, Complex patterns of divergence among green-sensitive (RH2a) African cichlid opsins revealed by Clade model analyses. *BMC Evol. Biol.* **12**, (2012).
46. L. G. Fogg, F. Cortesi, D. Lecchini, C. Gache, N. J. Marshall, F. de Busserolles, Development of dim-light vision in the nocturnal reef fish family Holocentridae I: Retinal gene expression. *J. Exp. Biol.* **225**, jeb244513 (2022).
47. K. E. O'Quin, C. M. Hofmann, H. A. Hofmann, K. L. Carleton, K. E. O'Quin, C. M. Hofmann, H. A. Hofmann, K. L. Carleton, Parallel evolution of opsin gene expression in african cichlid fishes. *Mol. Biol. Evol.* **27**, 2839–2854 (2010).
48. C. M. Hofmann, K. E. O'Quin, N. J. Marshall, T. W. Cronin, O. Seehausen, K. L. Carleton, The eyes have it: Regulatory and structural changes both underlie cichlid visual pigment diversity. *PLOS Biol.* **7**, e1000266 (2009).
49. M. Tobler, S. W. Coleman, B. D. Perkins, G. G. Rosenthal, Reduced opsin gene expression in a cave-dwelling fish. *Biol. Lett.* **6**, 98–101 (2010).
50. G. Fryer, T. D. Iles, *The Cichlid Fishes of the Great Lakes of Africa. Their Biology and Evolution* (Oliver and Boyd, 1972).
51. W. Salzburger, Understanding explosive diversification through cichlid fish genomics. *Nat. Rev. Genet.* **19**, 705–717 (2018).
52. F. Ronco, M. Matschiner, A. Böhne, A. Boila, H. H. Büscher, A. El Taher, A. Indermaur, M. Malinsky, V. Ricci, A. Kahmen, S. Jentoft, W. Salzburger, Drivers and dynamics of a massive adaptive radiation in cichlid fishes. *Nature* **589**, 76–81 (2021).
53. F. Ronco, H. H. Büscher, A. Indermaur, W. Salzburger, The taxonomic diversity of the cichlid fish fauna of ancient Lake Tanganyika, East Africa. *J. Great Lakes Res.* **46**, 1067–1078 (2020).
54. T. C. Spady, J. W. L. Parry, P. R. Robinson, D. M. Hunt, J. K. Bowmaker, K. L. Carleton, Evolution of the cichlid visual palette through ontogenetic subfunctionalization of the opsin gene arrays. *Mol. Biol. Evol.* **23**, 1538–1547 (2006).
55. V. I. Govardovskii, N. Fyhrquist, T. Reuter, D. G. Kuzmin, K. Donner, In search of the visual pigment template. *Vis. Neurosci.* **17**, 509–528 (2000).
56. K. L. Carleton, C. M. Hofmann, C. Klisz, Z. Patel, L. M. Chircus, L. H. Simenauer, N. Soodoo, R. C. Albertson, J. R. Ser, Genetic basis of differential opsin gene expression in cichlid fishes. *J. Evol. Biol.* **23**, 840–853 (2010).
57. J. Torres-Dowdall, N. Karagic, A. Härer, A. Meyer, Diversity in visual sensitivity across Neotropical cichlid fishes via.pdf. *Mol. Ecol.* **30**, 1180–1891 (2021).
58. I. Irisarri, P. Singh, S. Koblmüller, J. Torres-Dowdall, F. Henning, P. Franchini, C. Fischer, A. R. Lemmon, E. M. Lemmon, G. G. Thallinger, C. Sturmbauer, A. Meyer, Phylogenomics uncovers early hybridization and adaptive loci shaping the radiation of Lake Tanganyika cichlid fishes. *Nat. Commun.* **9**, 3159 (2018).
59. A. El Taher, A. Böhne, N. Boileau, F. Ronco, A. Indermaur, L. Widmer, W. Salzburger, Gene expression dynamics during rapid organismal diversification in African cichlid fishes. *Nat. Ecol. Evol.* **5**, 243–250 (2021).
60. W. Salzburger, T. Mack, E. Verheyen, A. Meyer, Out of Tanganyika: Genesis, explosive speciation, key-innovations and phylogeography of the haplochromine cichlid fishes. *BMC Evol. Biol.* **5**, 17 (2005).
61. C. Hahn, M. J. Genner, G. F. Turner, D. A. Joyce, The genomic basis of cichlid fish adaptation within the deepwater "twilight zone" of Lake Malawi. *Evol. Lett.* **1**, 184–198 (2017).
62. M. Malinsky, H. Svardal, A. M. Tyers, E. A. Miska, M. J. Genner, G. F. Turner, R. Durbin, Whole-genome sequences of Malawi cichlids reveal multiple radiations interconnected by gene flow. *Nat. Ecol. Evol.* **2**, 1940–1955 (2018).
63. C. Damsgaard, H. Lauridsen, A. M. D. Funder, J. S. Thomsen, T. Desvignes, D. A. Crossley, P. R. Møller, D. T. T. Huong, N. T. Phuong, H. W. Detrich, A. Brüel, H. Wilkens, E. Warrant, T. Wang, J. R. Nyengaard, M. Berenbrink, M. Bayley, Retinal oxygen supply shaped the functional evolution of the vertebrate eye. *eLife* **8**, e52153 (2019).
64. C. Damsgaard, H. Lauridsen, T. S. Harter, G. T. Kwan, J. S. Thomsen, A. M. D. Funder, C. T. Supuran, M. Tresguerres, P. G. D. Matthews, C. J. Brauner, A novel acidification mechanism for greatly enhanced oxygen supply to the fish retina. *eLife* **9**, e58995 (2020).
65. Y. Alvarez, M. L. Cederlund, D. C. Cottell, B. R. Bill, S. C. Ekker, J. Torres-Vazquez, B. M. Weinstein, D. R. Hyde, T. S. Vihtelic, B. N. Kennedy, Genetic determinants of hyaloid and retinal vasculature in zebrafish. *BMC Dev. Biol.* **7**, 114 (2007).
66. I. A. Frøland Steindal, D. Whitmore, Circadian clocks in fish-what have we learned so far? *Biology (Basel).* **8**, 17 (2019).
67. R. Feuda, A. K. Menon, M. C. Göpfert, Rethinking opsins. *Mol. Biol. Evol.* **39**, msac033 (2022).
68. K. L. Carleton, B. E. Dalton, D. Escobar-Camacho, S. P. Nandamuri, Proximate and ultimate causes of variable visual sensitivities: Insights from cichlid fish radiations. *Genesis* **54**, 299–325 (2016).
69. B. E. Dalton, E. R. Loew, T. W. Cronin, K. L. Carleton, Spectral tuning by opsin coexpression in retinal regions that view different parts of the visual field. *Proc. R. Soc. B Biol. Sci.* **281**, 20141980 (2014).
70. C. M. Hofmann, K. L. Carleton, Gene duplication and differential gene expression play an important role in the diversification of visual pigments in fish. *Integr. Comp. Biol.* **49**, 630–643 (2009).
71. D. Brawand, M. Soumillon, A. Necsulea, P. Julien, G. Csárdi, P. Harrigan, M. Weier, A. Liechti, A. Aximu-Petri, M. Kircher, F. W. Albert, U. Zeller, P. Khaitovich, F. Grützner, S. Bergmann, R. Nielsen, S. Pääbo, H. Kaessmann, The evolution of gene expression levels in mammalian organs. *Nature* **478**, 343–348 (2011).
72. M. Malinsky, R. J. Challis, A. M. Tyers, S. Schiffels, Y. Terai, B. P. Ngatunga, E. A. Miska, R. Durbin, M. J. Genner, G. F. Turner, Genomic islands of speciation separate cichlid ecomorphs in an East African crater lake. *Science* **350**, 1493–1498 (2015).
73. H. Nagai, Y. Terai, T. Sugawara, H. Imai, H. Nishihara, M. Hori, N. Okada, Reverse evolution in RH1 for adaptation of cichlids to water depth in Lake Tanganyika. *Mol. Biol. Evol.* **28**, 1769–1776 (2011).
74. R. Jordan, D. Howe, F. Juanes, J. J. Stauffer Jr., E. Loew, Ultraviolet radiation enhances zooplanktivory rate in ultraviolet sensitive cichlids. *Afr. J. Ecol.* **42**, 228–231 (2004).
75. H. I. Browman, I. Novales-Flamarique, C. W. Hawryshyn, Ultraviolet photoreception contributes to prey search behaviour in two species of zooplanktivorous fishes. *J. Exp. Biol.* **186**, 187–198 (1994).
76. F. Ronco, W. Salzburger, Tracing evolutionary decoupling of oral and pharyngeal jaws in cichlid fishes. *Evol. Lett.* **5**, 625–635 (2021).
77. A. El Taher, F. Ronco, M. Matschiner, W. Salzburger, A. Böhne, Dynamics of sex chromosome evolution in a rapid radiation of cichlid fishes. *Sci. Adv.* **7**, eabe8215 (2021).
78. A. M. Bolger, M. Lohse, B. Usadel, Trimmomatic: A flexible trimmer for Illumina sequence data. *Bioinformatics* **30**, 2114–2120 (2014).
79. A. Dobin, C. A. Davis, F. Schlesinger, J. Drenkow, C. Zaleski, S. Jha, P. Batut, M. Chaisson, T. R. Gingeras, STAR: Ultrafast universal RNA-seq aligner. *Bioinformatics* **29**, 15–21 (2013).
80. S. Anders, P. T. Pyl, W. Huber, HTSeq-A Python framework to work with high-throughput sequencing data. *Bioinformatics* **31**, 166–169 (2015).
81. A. Necsulea, H. Kaessmann, Evolutionary dynamics of coding and non-coding transcriptomes. *Nat. Rev. Genet.* **15**, 734–748 (2014).
82. M. I. Love, W. Huber, S. Anders, Moderated estimation of fold change and dispersion for RNA-seq data with DESeq2. *Genome Biol.* **15**, 550 (2014).
83. R Core Team, *R: A Language and Environment for Statistical Computing* (R Foundation for Statistical Computing, 2022).
84. L. J. Revell, phytools: An R package for phylogenetic comparative biology (and other things). *Methods Ecol. Evol.* **3**, 217–223 (2012).
85. E. Paradis, J. Claude, K. Strimmer, APE: Analyses of phylogenetics and evolution in R language. *Bioinformatics* **20**, 289–290 (2004).
86. S. W. Kembel, P. D. Cowan, M. R. Helmus, W. K. Cornwell, H. Morlon, D. D. Ackerly, S. P. Blomberg, C. O. Webb, Picante: R tools for integrating phylogenies and ecology. *Bioinformatics* **26**, 1463–1464 (2010).
87. K. L. Carleton, T. C. Spady, J. T. Streelman, M. R. Kidd, W. N. McFarland, E. R. Loew, Visual sensitivities tuned by heterochronic shifts in opsin gene expression. *BMC Biol.* **6**, 22 (2008).
88. D. Orme, The caper package: Comparative analysis of phylogenetics and evolution in R. R Package version 0.5, 2 (2013).

89. D. C. Adams, E. Otárola-Castillo, Geomorph: An R package for the collection and analysis of geometric morphometric shape data. *Methods Ecol. Evol.* **4**, 393–399 (2013).

Acknowledgments: We thank A. El Taher, A. Indermaur, and L. Widmer for assistance in the field; A. Irakoze, G. Katai, G. Kazumbe, D. Mwanakulya, J. Sichilima, and H. D. Sichilima Jr. for help and support during field work; G. Banyankimbona (Burundi), L. Makasa (Zambia), and M. Mukuli (Tanzania) for help with obtaining researcher permits; F. Cortesi, A. El Taher, A. Fages, L. Fogg, Z. Musilova, M. Policarpo, and P. Tschopp for valuable feedback and/or discussions; S. Stieb for the demonstration of retina dissection; C. Huyghe for help with retina dissection; and the Genomics Facility Basel (ETH Zurich) for sequencing our RNA samples. Calculations were performed at sciCORE (https://scicore.unibas.ch/), the Center for Scientific Computing at the University of Basel, with support by the Swiss Institute of Bioinformatics (SIB). **Funding:** This work was funded by grants from the European Research Council (ERC, CoG number 617585 "CICHLID~X") and the Swiss National Science Foundation (SNSF) to W.S. (numbers 176039 and 208002) and F.R. (number 206869). **Author contributions:** Experimental design: V.R. and W.S. Sampling and field work: V.R., N.B., F.R., and W.S. Retina dissection and RNA extraction: V.R. and N.B. Gene expression analyses: V.R. Comparative analyses: V.R. and F.R. Supervision: F.R. and W.S. Writing—original draft: V.R. and W.S. Writing—review and editing: V.R., W.S., F.R., and N.B.

Competing interests: The authors declare that they have no competing interests. **Data and materials availability:** The raw read data are available from NCBI under the BioProject accession number PRJNA913112. The raw read count table has been uploaded in the Supplementary Materials (data S1). Data and custom scripts have been deposited on Dryad (https://datadryad.org/stash/dataset/doi:10.5061/dryad.r2280gbj2) and on GitHub (https://github.com/Ninet93/RNASeq_Ricci_et_al.git). The time-calibrated species tree, raw genome sequencing data (NCBI BioProject accession no. PRJNA550295), gene duplication and positive selection analyses, stable carbon (C) and nitrogen (N) isotope signatures, and relative eye size data were taken from Ronco *et al.* (*52*) (data available on Dryad: https://datadryad.org/stash/dataset/doi:10.5061/dryad.9w0vt4bbf). The habitat categories were taken from Ricci *et al.* (*30*) (data available on Dryad: https://datadryad.org/stash/dataset/doi:10.5061/dryad.4mw6m90c7). All data needed to evaluate the conclusions in the paper are present in the paper and/or the Supplementary Materials.

Submitted 17 January 2023
Accepted 7 August 2023
Published 6 September 2023
10.1126/sciadv.adg6568

ScienceAdvances

Visual opsin gene expression evolution in the adaptive radiation of cichlid fishes of Lake Tanganyika

Virginie Ricci, Fabrizia Ronco, Nicolas Boileau, and Walter Salzburger

Sci. Adv. **9** (36), eadg6568. DOI: 10.1126/sciadv.adg6568

Science Advances (ISSN 2375-2548) is published by the American Association for the Advancement of Science. 1200 New York Avenue NW, Washington, DC 20005. The title *Science Advances* is a registered trademark of AAAS.